Ab initio calculations on the 2B1 and 2A1 states of AsH2, and Franck–Condon simulation, including anharmonicity, of the (0,0,0)-single vibronic level emission spectrum of AsH2

Edmond P. F. Lee, Daniel K. W. Mok, Foo-tim Chau, and John M. Dyke

Citation: J. Chem. Phys. **132**, 234309 (2010); doi: 10.1063/1.3442748
View online: http://dx.doi.org/10.1063/1.3442748
View Table of Contents: http://jcp.aip.org/resource/1/JCPSA6/v132/i23
Published by the American Institute of Physics.

Related Articles

Electronic transitions of cobalt monoboride
J. Chem. Phys. 135, 204308 (2011)

The electronic spectrum of the previously unknown HAsO transient molecule
J. Chem. Phys. 135, 184308 (2011)

Rotational temperature analysis of N2 by resonant enhanced multi-photon ionization with fluorescence detection
J. Appl. Phys. 110, 083309 (2011)

Theoretical investigation of the photophysics of methyl salicylate isomers
J. Chem. Phys. 135, 164306 (2011)

Laser-induced fluorescence studies of HfF+ produced by autoionization
J. Chem. Phys. 135, 154308 (2011)

Additional information on J. Chem. Phys.

Journal Homepage: http://jcp.aip.org/
Journal Information: http://jcp.aip.org/about/about_the_journal
Top downloads: http://jcp.aip.org/features/most_downloaded
Information for Authors: http://jcp.aip.org/authors

ADVERTISEMENT

Downloaded 10 Jan 2012 to 158.132.161.9. Redistribution subject to AIP license or copyright; see http://jcp.aip.org/about/rights_and_permissions

Ab initio calculations on the $\tilde{X}\ ^2B_1$ and $\tilde{A}\ ^2A_1$ states of AsH_2, and Franck–Condon simulation, including anharmonicity, of the $\tilde{A}(0,0,0)$-$\tilde{X}$ single vibronic level emission spectrum of AsH_2

Edmond P. F. Lee,[1,a)] Daniel K. W. Mok,[1,b)] Foo-tim Chau,[1,b)] and John M. Dyke[2]
[1]*Department of Applied Biology and Chemical Technology, The Hong Kong Polytechnic University, Hung Hom, Hong Kong*
[2]*School of Chemistry, University of Southampton, Highfield, Southampton SO17 1BJ, United Kingdom*

(Received 28 December 2009; accepted 12 May 2010; published online 17 June 2010)

Restricted-spin coupled-cluster single-double plus perturbative triple excitation {RCCSD(T)} calculations were carried out on the $\tilde{X}\ ^2B_1$ and $\tilde{A}\ ^2A_1$ states of AsH_2 employing the fully relativistic small-core effective core potential (ECP10MDF) for As and basis sets of up to the augmented correlation-consistent polarized valence quintuple-zeta (aug-cc-pV5Z) quality. Minimum-energy geometrical parameters and relative electronic energies were evaluated, including contributions from extrapolation to the complete basis set limit and from outer core correlation of the As $3d^{10}$ electrons employing additional tight 4d3f2g2h functions designed for As. In addition, simplified, explicitly correlated CCSD(T)-F12 calculations were also performed employing different atomic orbital basis sets of up to aug-cc-pVQZ quality, and associated complementary auxiliary and density-fitting basis sets. The best theoretical estimate of the relative electronic energy of the $\tilde{A}\ ^2A_1$ state of AsH_2 relative to the $\tilde{X}\ ^2B_1$ state including zero-point energy correction (T_0) is 19 954(32) cm^{-1}, which agrees very well with available experimental T_0 values of 19 909.4531(18) and 19 909.4910(17) cm^{-1} obtained from recent laser induced fluorescence and cavity ringdown absorption spectroscopic studies. In addition, potential energy functions (PEFs) of the $\tilde{X}\ ^2B_1$ and $\tilde{A}\ ^2A_1$ states of AsH_2 were computed at different RCCSD(T) and CCSD(T)-F12 levels. These PEFs were used in variational calculations of anharmonic vibrational wave functions, which were then utilized to calculate Franck–Condon factors (FCFs) between these two states, using a method which includes allowance for anharmonicity and Duschinsky rotation. The $\tilde{A}(0,0,0)$-$\tilde{X}$ single vibronic level (SVL) emission spectrum of AsH_2 was simulated using these computed FCFs. Comparison between simulated and available experimental vibrationally resolved spectra of the $\tilde{A}(0,0,0)$-$\tilde{X}$ SVL emission of AsH_2, which consist essentially of the bending (2_n) series, suggests that there is a significant loss in intensity in the low emission energy region of the experimental spectrum.
© *2010 American Institute of Physics*. [doi:10.1063/1.3442748]

I. INTRODUCTION

AsH_2 is important as an intermediate in chemical vapor etching of gallium arsenide (GaAs) in the semiconductor industry, when arsine (AsH_3) is used as a precursor.[1–3] This has provided a stimulus for various spectroscopic investigations, which include absorption,[4] emission,[5] microwave (MW),[6,7] far infrared laser magnetic resonance (FIR-LMR),[3] laser induced fluorescence (LIF),[8] dispersed fluorescence {or single vibronic level (SVL) emission}[8] and cavity ringdown (CRD) absorption[9] spectroscopic studies (detailed discussions on previous spectroscopic studies on AsH_2 can be found in Refs. 3, 8, and 9, and hence they will not be repeated here). On the computational front, some *ab initio* studies[8,10–14] have been made on AsH_2, and, also, two high-level, scalar relativistic studies have recently been published on AsH_2^+. They involve third order Douglas-Kroll coupled-cluster single-double-triple-quadruple excitation (DK3-CCSDTQ) (Ref. 15) and active space DK3-CCSDTq (Ref. 16) calculations. However, the highest level *ab initio* calculations performed previously on the $\tilde{X}\ ^2B_1$ and $\tilde{A}\ ^2A_1$ states of AsH_2 are the coupled-cluster single-double plus perturbative triple excitation {CCSD(T)} calculations described in Ref. 8, which employed the augmented correlation-consistent polarized-valence quadruple-zeta (aug-cc-pVQZ) basis set. In the present study, we propose to carry out higher level *ab initio* calculations on the $\tilde{X}\ ^2B_1$ and $\tilde{A}\ ^2A_1$ states of AsH_2, which include considerations of scalar relativistic effects and outer core correlation in As and extrapolation to the complete basis set (CBS) limit. We also proposed to use explicit correlation methods (*vide infra*). In addition, we propose to carry out spectral simulations on the $\tilde{A}(0,0,0)$-$\tilde{X}$ SVL emission spectrum of AsH_2, based on computed Franck–Condon (FC) factors, which include allowance for anharmonicity and

[a)]Also at Southampton.
[b)]Authors to whom correspondence should be addressed. Electronic addresses: bcdaniel@polyu.edu.hk and bcftchau@polyu.edu.hk.

 © 2010 American Institute of Physics

Downloaded 10 Jan 2012 to 158.132.161.9. Redistribution subject to AIP license or copyright; see http://jcp.aip.org/about/rights_and_permissions

TABLE I. Basis sets used for AsH_2.

Label	As	Frozen core[a]	H	Nbasis[b]
AVTZ	ECP10MDF_aug-cc-pVTZ[c]	As $3s^23p^63d^{10}$	Aug-cc-pVTZ	101
ACVTZ	ECP10MDF_aug-cc-pVTZ+3d2f [d]	As $3s^23p^6$	Aug-cc-pVTZ	130
AVQZ	ECP10MDF_aug-cc-pVQZ	As $3s^23p^63d^{10}$	Aug-cc-pVQZ	181
AV5Z	ECP10MDF_aug-cc-pV5Z	As $3s^23p^63d^{10}$	Aug-cc-pV5Z	296
ACV5Z	ECP10MDF_aug-cc-pV5Z+4d3f2g2h [e]	As $3s^23p^6$	Aug-cc-pV5Z	377
$AVTZ_{ae}$	Aug-cc-pVTZ[f]	Default As core	Aug-cc-pVTZ	105
$AVQZ_{ae}$	Aug-cc-pVQZ[g]	Default As core	Aug-cc-pVQZ	185

[a]These electrons were kept frozen in the RCCSD(T) or UCCSD(T)-F12x calculations.
[b]Nbasis is the total number of contracted Gaussian functions used for AsH_2.
[c]The ECP10MDF_aug-cc-pVTZ and aug-cc-pVTZ AO bases for As and H, respectively, were used with the RI(R)-basis of cc-pVTZ/JKFIT (number of functions=244) and DF-basis of aug-cc-pVTZ/MP2FIT (number of functions=283) in the UCCSD(T)-F12x calculations (see text, and also Refs. 24 and 26).
[d]The ECP10MDF_aug-cc-pVTZ AO basis for As was augmented with 3d (exponents: 13.5, 4.5, 1.5) and 2f (exponents: 7.5, 2.5) tight functions in order to account for the As $3d^{10}$ outer core electrons adequately. The RI(R)-basis of cc-pVTZ/JKFIT (number of functions=244) and DF-basis of aug-cc-pVTZ/MP2FIT (number of functions=283) were used in the UCCSD(T)-F12x calculations (see text, and also Refs. 24 and 26).
[e]The augmented 4d3f2g2h functions designed to account for the As $3d^{10}$ outer core electrons have the following exponents: 4d (18.4, 9.2, 4.6, and 2.3), 3f (12.0, 4.8, and 1.92), 2g (7.2 and 2.4), and 2h (8.575 and 2.45).
[f]The all electron (denoted by the subscript ae) aug-cc-pVTZ AO basis, the default RI(R)-basis of cc-pVTZ/JKFIT (number of functions=244) and DF-basis of aug-cc-pVTZ/MP2FIT (number of functions=283) were used in the UCCSD(T)-F12x calculations (see text, and also Refs. 24 and 26).
[g]The all electron (denoted by the subscript ae) aug-cc-pVQZ AO basis, the default RI(R)-basis of cc-pVQZ/JKFIT (number of functions=297) and DF-basis of aug-cc-pVQZ/MP2FIT (number of functions=422) were used in the UCCSD(T)-F12x calculations (see text, and also Refs. 24 and 26).

Duschinsky rotation. The experimental $\tilde{A}(0,0,0)$-$\tilde{X}$ SVL emission spectrum of AsH_2 has been recorded recently.[8] As will be discussed, comparison between simulated and experimental spectra suggests a significant loss in intensity in the low emission energy region of the experimental spectrum.

II. THEORETICAL CONSIDERATIONS AND COMPUTATIONAL DETAILS

Geometry optimization and harmonic vibrational frequency calculations were carried out on the $\tilde{X}\ ^2B_1$ and $\tilde{A}\ ^2A_1$ states of AsH_2 employing the restricted-spin coupled-cluster single and double plus perturbative triple excitations {RCCSD(T)} method[17] as implemented in the MOLPRO suite of programs.[18] Basis sets of different qualities have been used and they are summarized in Table I. Specifically, the fully relativistic small-core effective core potential (ECP), ECP10MDF,[19] and associated augmented correlation-consistent polarized valence quadruple- and quintuple-zeta basis sets (aug-cc-pVQZ_PP and aug-cc-pV5Z_PP) (Ref. 20) were used for As [see Table I for the corresponding basis sets used for H (Ref. 21)]. In addition to accounting for the $1s^22s^22p^6$ core electrons of As, the fully relativistic ECP10MDF ECP also accounts for scalar relativistic contributions from As. Regarding outer core correlation, the As $3d^{10}$ electrons were correlated explicitly in the RCCSD(T) calculations, employing the aug-cc-pV5Z_PP basis set for As and with additional tight 4d3f2g2h functions designed to account for the As $3d^{10}$ electrons adequately (labeled as ACV5Z throughout; see Table I and footnote e). From our previous investigation on low-lying electronic states of SbO_2, it was found that, while effects of outer core correlation of the Sb $4d^{10}$ electrons on optimized geometrical parameters and computed relative electronic energies are considerable, core correlation effects arising from the Sb $4s^24p^6$ electrons are insignificantly small.[22] Since As is above Sb in the Periodic Table, core correlation effects of the As $3s^23p^6$ electrons on computed molecular properties are expected to be weaker than those of the Sb $4s^24p^6$ electrons, because the energy separations between the outer core 3s3p shells and the valence 4s4p shells of As are larger than the corresponding separations between the outer core 4s4p shells and the valence 5s5p shells of Sb. In view of the above considerations, it is concluded that including only outer core correlation of As $3d^{10}$ electrons in the present study on AsH_2 should be adequate. Lastly, extrapolations of optimized geometrical parameters and computed relative electronic energies to the CBS limit were carried out employing the two point extrapolation technique of the form, $1/X^3$.[23] In obtaining the best theoretical estimates of these computed quantities, it has been assumed that contributions arising from outer core correlation of As and extrapolation to the CBS limit are additive.

In addition to RCCSD(T) calculations described above, we have also carried out geometry optimization and harmonic vibrational frequency calculations on the $\tilde{X}\ ^2B_1$ and $\tilde{A}\ ^2A_1$ states of AsH_2 using explicitly correlated coupled cluster methods based on the recently reported, simplified UCCSD-F12x approximations.[24] The historical development of explicit correlation methods has been reviewed recently,[25] and the F12 approach (F12 denotes a nonlinear correlation factor cf. a linear correlation factor as used in the R12 approach; see Refs. 24 and 25) has been incorporated into the MP2 (Møller–Plesset theory to the second order) and CCSD theory (see Refs. 24 and 25, and references therein). In the present study, the simplified RHF/UCCSD(T)-F12x (x=a or b; see Ref. 24 and MOLPRO online user manual[26] for details, and the acronyms used) methods, as implemented in MOLPRO, have been employed. The atomic orbital (AO) basis sets, associated complementary auxiliary basis sets {CABS for resolution of identity (RI) approximations} and density fitting (DF) basis sets used in these UCCSD(T)-F12x (x=a or b) calculations are also given in Table I (see footnotes c, d, f, and g). Most of the default options (e.g., the wave function ansatz, RI approximation, CABS, and DF basis sets) as rec-

Downloaded 10 Jan 2012 to 158.132.161.9. Redistribution subject to AIP license or copyright; see http://jcp.aip.org/about/rights_and_permissions

TABLE II. Some technical details for the PEFs obtained using computed RCCSD(T)/AV5Z, RCCSD(T)/ACV5Z and RHF/UCCSD(T_{sc})-F12a/ACVTZ energy points, and for variational calculations of anharmonic vibrational wave functions, of the $\tilde{X}\ ^2B_1$ and $\tilde{A}\ ^2A_1$ state of AsH_2.

	RCCSD(T)/AV5Z		RCCSD(T)/ACV5Z		UCCSD(T_{sc})-F12a	
PEF fitting	$\tilde{X}\ ^2B_1$	$\tilde{A}\ ^2A_1$	$\tilde{X}\ ^2B_1$	$\tilde{A}\ ^2A_1$	$\tilde{X}\ ^2B_1$	$\tilde{A}\ ^2A_1$
r(AsH)/Å	$1.1 \le r \le 2.1$	$1.0 \le r \le 2.1$	$1.15 \le r \le 2.3$	$1.15 \le r \le 2.3$	$1.0 \le r \le 2.25$	$1.05 \le r \le 2.25$
θ(HAsH)/°	$65 \le \theta \le 165$	$60 \le \theta \le 167$	$55 \le \theta \le 155$	$67 \le \theta \le 167$	$60 \le \theta \le 160$	$65 \le \theta \le 165$
Energy points	139	138	138	113	149	134
rms deviation/cm^{-1}	5.6	9.4	4.9	9.1	6.7	5.1
			Variational calculations[a]			
Max. v_1	5	5	8	10	8	8
Max. v_2	20	20	20	20	20	20
Max. (v_1+v_2)	20	20	20	20	20	20

[a]v_1 and v_2 refer to vibrational quantum numbers of harmonic basis functions of the symmetric stretching and bend modes, respectively.

ommended by the authors of MOLPRO (see Refs. 24 and 26) have been used. Nevertheless, the following points should be noted. First, although the computed contributions of perturbative triple excitations in the UCCSD(T)-F12x approach do not have a direct F12 correction, a simple and pragmatic improvement of the triples energy by the scaling factor, $E_{corr}^{MP2\text{-}F12}/E_{corr}^{MP2}$ (i.e., the ratio between the computed correlation energies obtained at the MP2 and MP2-F12 levels), has been proposed.[24,26] In this connection, in the following discussion, (T_{sc}) denotes scaled triples obtained in this way {i.e., $\Delta E(T_{sc}) = \Delta E(T) \times E_{corr}^{MP2\text{-}F12}/E_{corr}^{MP2}$}. {Note that in the following text, when UCCSD(T)-F12x is used, it refers generally to calculations employing scaled or unscaled triples and also use of the x=a or b methods.[24] Otherwise, the specific choices of triples and x will be given. Also, in all cases, the restricted-spin Hartree–Fock (RHF) wave function is used as the reference wave function in subsequent UCCSD(T)-F12x calculations as implemented in MOLPRO.} Although it was found that computed scaling factors can have values larger or smaller than 1, they are quite close to 1 in most cases. As a result, the differences between using scaled or unscaled triples were found to be insignificantly small (*vide infra*). Second, with the AVTZ and ACVTZ basis sets, which are basis sets associated with the ECP10MDF ECP (see Table I), the CABS and DF basis sets used in the UCCSD(T)-F12x calculations carried out in the present study are the same as those used with the all-electron $AVTZ_{ae}$ basis set (see footnotes c and d of Table I). As will be discussed below, the results obtained suggest that these CABS and DF basis sets are suitable and adequate for the ECP AO basis set used. Third, benchmark UCCSD(T)-F12x calculations very recently reported in Ref. 24 have not considered core electrons, ECP basis sets and third row elements, which have been investigated in the present study.

The fitting of potential energy functions (PEFs) of the two electronic states involved, variational calculations of anharmonic vibrational wave functions, and FC factor calculations employing computed anharmonic vibrational wave functions and including allowance for Duschinsky rotation have been described previously,[27,28] and hence will not be repeated here. Nevertheless, some technical details specific to the present studies are summarized in Table II. It should be noted that three different sets of PEFs for the two states considered have been obtained by employing three different sets of computed energies; they are:-RCCSD(T)/AV5Z, RCCSD(T)/ACV5Z and RHF/UCCSD(T_{sc})-F12a/ACVTZ (see Table II; *vide infra*). Regarding the harmonic basis functions used in the variational calculations of anharmonic vibrational wave functions (which are expressed in terms of linear combinations of harmonic basis functions; see Ref. 28), different harmonic basis sets {i.e., with different maximum v_1, v_2 and/or (v_1+v_2) values; see footnote a of Table II} have been employed. Nevertheless, vibrational basis size effects on the computed anharmonic vibrational energies and wave functions were found to be negligibly small.

It should be noted that for the ranges of geometrical parameters of the two electronic states considered (Table II), the computed T_1 diagnostics obtained from all RCCSD and UCCSD calculations carried out have values smaller than 0.025, indicating that there is negligible multireference (MR) character in these regions of the PEFs, and hence the single reference CCSD(T) method is appropriate. In order to confirm this, further CASSCF/ECP10MDF_aug-cc-pVTZ,aug-cc-pVTZ calculations with a full valence active space have been carried out at selected geometries of both states {r values from 1.1 to 2.3 Å with θ having values of 90.8° and 122.0° (the widest range of r values used in the energy scans for the PEFs was with these θ_e values of the two states), and θ values from 55° to 167° with r having the value of 1.5 Å (the widest range of θ values used in the energy scans for the PEFs was with the r_e values of the two states)}. For the whole range of θ values considered, the CASSCF CI coefficients of the main electronic configurations (C_{main}) of the two states have computed values of larger than 0.97. For r having values between 1.1 and 2.1 Å, all computed C_{main} values of the two states are larger than 0.909. For the $\tilde{X}\ ^2B_1$ state, at r=2.2 and 2.3 Å, the computed C_{main} values are 0.908 and 0.884, and for the $\tilde{A}\ ^2A_1$ state, the computed C_{main} values are 0.852 and 0.790, respectively. Summarizing, for the bending coordinate considered, there is hardly any MR character in the region covered by the energy scans of the PEFs of the two states. For the symmetric stretching coordinate considered, MR character is negligibly small within the r=1.1 to 2.1 Å region, and there is only a slight amount of MR character with r values larger than 2.1 Å (mainly for the

Downloaded 10 Jan 2012 to 158.132.161.9. Redistribution subject to AIP license or copyright; see http://jcp.aip.org/about/rights_and_permissions

$\tilde{A}\ ^2A_1$ state). In any case, since the geometry difference between the two states concerned is mainly in the bond angle, vibrational excitations are essentially in the bending mode, whether upon excitation or deexcitation, and the involvement of the symmetric stretching mode is very weak, as shown in the experimental SVL emission spectrum to be discussed below. In this connection, it is concluded that the PEFs employed in the present study are adequate for the purpose.

In simulation of the $\tilde{A}\ ^2A_1(0,0,0) \rightarrow \tilde{X}\ ^2B_1$ SVL emission spectrum of AsH_2, vibrational components were simulated using Gaussian functions with a full-width-at-half-maximum (FWHM) of 5 cm^{-1}. The relative intensity of each vibrational component in a simulated SVL emission spectrum was expressed as the product of the corresponding computed anharmonic FC factor and a frequency factor of power 4. In simulated SVL emission spectra, the energy scale in wavenumber (cm^{-1}) is taken relative to the laser excitation line, i.e., the displacement energy from the excitation frequency toward lower emission energy (hence it is a negative number; note that in published experimental dispersed fluorescence spectra, the energy axis usually gives the displacement energy as a direct measure of the ground electronic state vibrational energy, hence is a positive number).

III. RESULTS AND DISCUSSIONS

Ab initio computed values are summarized and compared with experimental values, where available, in Tables III–VII. Some representative simulated spectra are given in Figs. 1–3. Computed geometrical parameters, vibrational frequencies and relative electronic energies of the $\tilde{X}\ ^2B_1$ and $\tilde{A}\ ^2A_1$ states of AsH_2 will be discussed first, before the simulated spectra are presented and discussed.

IV. OPTIMIZED GEOMETRICAL PARAMETERS OF THE $\tilde{X}\ ^2B_1$ STATE OF AsH_2

From Table III, it can be seen that with the RCCSD(T) method, basis set size effects {differences between RCCSD(T)/AVQZ and RCCSD(T)/AV5Z results} on the computed equilibrium bond lengths and angles of the $\tilde{X}\ ^2B_1$ state of AsH_2 are insignificantly small, when basis sets of AVQZ and AV5Z qualities are used. Core correlation effects (differences between AV5Z and ACV5Z results) are slightly larger on the optimized bond length than basis set size effects, but are negligibly small for the computed bond angle. The best estimated equilibrium geometrical parameters for the $\tilde{X}\ ^2B_1$ state of AsH_2 obtained in the present study are $r_e(AsH) = 1.5118 \pm 0.0002$ Å and $\theta_e(HAsH) = 90.89° \pm 0.01°$ (see footnote c of Table III). When these best estimated values are compared with available experimentally derived r_e values of 1.5249 Å and 90.765° from the CRD study of Ref. 9, and 1.5158 ± 0.0006 Å and $90.79° \pm 0.08°$ from the MW study of Ref. 7, the agreement between theory and experiment in the equilibrium bond angle, θ_e, is found to be within 0.13°, which is very good. For the equilibrium bond length, r_e, the agreement between the best estimated value obtained here and the experimental value derived from the MW study is within 0.004 Å, which is also very good. However, the agreement with the experimentally derived value from the CRD study is not as good (difference 0.013 Å). Our best estimated r_e value favors the experimental r_e value derived from the MW study over that derived from the CRD study. Nevertheless, it should be noted that experimental r_e geometrical parameters are usually derived from experimental r_0 geometrical parameters (with corrections for centrifugal distortion and anharmonicities; see, for example, Ref. 29), and it has been noted in Ref. 8 that, there is no information on the ν_1 anharmonicity for the $\tilde{X}\ ^2B_1$ state of AsH_2, which is expected to be substantial, or on the value of ν_3 (the deficiency is even greater for the $\tilde{A}\ ^2A_1$ state of AsH_2). In this connection, the r_0 geometrical parameters and rotational constants of the $\tilde{X}\ ^2B_1$ state of AsH_2 have also been computed (from computed anharmonic vibrational wave functions). When the best estimated r_0 values ($r_0 = 1.5203$ Å, $\theta_0 = 90.94°$, $A_0 = 7.556$ cm^{-1}, $B_0 = 7.120$ cm^{-1}, and $C_0 = 3.666$ cm^{-1}; see Table III and footnote d) are compared with available, corresponding r_0 experimental values (approximately 1.518 Å, 90.74°, 7.550 cm^{-1}, 7.163 cm^{-1}, and 3.615–3.676 cm^{-1}; see Table III), it is pleasing to see that the agreement between theory and experiment is very good.

Considering the computed equilibrium geometrical parameters of the $\tilde{X}\ ^2B_1$ state of AsH_2 obtained employing the explicitly correlated UCCSD(T)-F12x methods, the following conclusions can be drawn based on the results shown in Table III. First, basis size effects (for example, differences between using the $AVTZ_{ae}$ and $AVQZ_{ae}$ basis sets) seem to be small. This is as expected for explicitly correlated methods, which can achieve a dramatic improvement of basis set convergence of correlation energies when compared with conventional correlation methods (e.g., results of a quintuple-zeta quality basis set using a conventional correlation method can be obtained with a triple-zeta quality basis set using an explicitly correlated method; see Ref. 24 and references therein). Second, based on results obtained from a systematic investigation using the AVTZ basis set, the differences between using the F12a or F12b approximation, and/or scaled (T_{sc}) or unscaled (T) triples are insignificantly small. Third, the largest differences in the optimized r_e values (decreases of approximately 0.01 Å) arise from including the As $3d^{10}$ core electrons in the correlation treatment (the differences between employing the ACVTZ and AVTZ basis sets). Fourth, the largest differences in the optimized θ_e values (differences of approximately 0.3°) arise from the use of ECP basis sets compared with use of all electron basis sets, suggesting that relativistic effects decrease the computed θ_e values slightly. In addition, the similar results obtained using ECP and all electron basis sets, and both RCCSD(T) and UCCSD(T)-F12x methods, suggest that the CABS and DF basis sets employed in UCCSD(T)-F12x calculations are suitable and adequate in all cases. Lastly, it is pleasing to see that the computed geometrical parameters (r_e and r_0 values) obtained at the UCCSD(T)-F12b/ACVTZ and UCCSD(T_{sc})-F12a/ACVTZ levels, with the As $3d^{10}$ core

Downloaded 10 Jan 2012 to 158.132.161.9. Redistribution subject to AIP license or copyright; see http://jcp.aip.org/about/rights_and_permissions

TABLE III. Computed minimum-energy geometrical parameters (r_e and θ_e in angstrom and degrees, respectively; r_0 values are specified under method) and the corresponding rotational constants (A, B, and C in cm^{-1}) of the $\tilde{X}\ ^2B_1$ state of AsH_2.

Method	r_e	θ_e	A	B	C
RCCSD(T)/AVQZ	1.5252	90.87			
RCCSD(T)/AV5Z	1.5250	90.89			
RCCSD(T)/ACV5Z	1.5120	90.87			
CBS[a]	1.5248	90.90			
Core[b]	−0.0130	−0.01			
Best estimate (CBS+Core) [c]	1.5118(2)	90.89(1)	7.633	7.207	3.707
RCCSD(T)/AV5Z PEF	1.5249	90.90	7.505	7.082	3.644
RCCSD(T)/AV5Z PEF r_0	1.5333	90.97	7.432	6.995	3.604
RCCSD(T)/ACV5Z PEF	1.5119	90.92	7.637	7.202	3.706
RCCSD(T)/ACV5Z PEF r_0	1.5204	90.97	7.559	7.115	3.665
Best r_0 [d]	1.5203	90.94	7.556	7.120	3.666
RHF/UCCSD(T)-F12b/$AVTZ_{ae}$	1.5287	91.07	7.490	7.025	3.625
RHF/UCCSD(T_{sc})-F12b/$AVQZ_{ae}$	1.5283	91.13	7.500	7.022	3.627
RHF/UCCSD(T_{sc})-F12a/AVTZ	1.5260	90.80	7.481	7.083	3.638
RHF/UCCSD(T)-F12a/AVTZ	1.5258	90.82			
RHF/UCCSD(T_{sc})-F12b/AVTZ	1.5260	90.79			
RHF/UCCSD(T)-F12b/AVTZ	1.5258	90.81			
RHF/UCCSD(T)-F12b/ACVTZ	1.5153	90.79			
RHF/UCCSD(T_{sc})-F12a/ACVTZ	1.5146	90.76	7.588	7.196	3.693
RHF/UCCSD(T_{sc})-F12a/ACVTZ PEF	1.5146	90.79			
(as above) r_0	1.5232	90.86	7.517	7.103	3.652
UCCSD(T)/aug-cc-pVQZ[e]	1.508	90.9			
Absorption r_0 [f]	1.518	90.73	7.5486	7.1624	3.6166
MW r_0 [g]			7.5501	7.1629	3.6148
MW (AsD_2, [h]) $r_z(AsH_2)$	1.53436(15)	90.695(20)			
MW (AsD_2, [h]) $r_e(AsH_2)$	1.5158(6)	90.79(8)			
FIR-LMR[i] r_0 [j]	1.518	90.746	7.5497	7.1629	3.6149
LIF[k] r_0 [l]	1.5183(1)	90.75(1)	7.550	7.162	3.676
CRD absorption[m]	1.5249	90.765			

[a]Extrapolation to the CBS limit using the $1/X^3$ formula and the RCCSD(T)/AVQZ and RCCSD(T)/AV5Z values.
[b]Contributions from As $3d^{10}$ outer core correlation take the difference between the computed RCCSD(T)/ACV5Z values, which include As $3d^{10}$ electrons in the correlation calculations, and the RCCSD(T)/AV5Z values, with the default frozen core.
[c]The best estimated values take the sums of the CBS values and Core contribution. The uncertainties are estimated by the difference between the best estimates and the RCCSD(T)/ACV5Z values.
[d]The best r_0 values are estimated by the sums of the best estimated r_e values and the differences between the r_0 and r_e values obtained from the RCCSD(T)/ACV5Z PEF.
[e]From Ref. 8, using G03.
[f]Reference 4.
[g]Reference 6.
[h]Reference 7.
[i]Reference 3.
[j]Using the r_0 geometrical parameters derived in the FIR-LMR study, the corresponding rotational constants, A_0, B_0, and C_0 were evaluated to be 7.552, 7.166, and 3.677 cm^{-1}. The set of A, B, and C values shown in the table are from Table III of Ref. 3 given for the v=0 level of the ground $^2B_1$ state of AsH_2. Another set of A_0, B_0, and C_0 values of 7.5468, 7.1629, and 3.6149 cm^{-1} were given in Table IV of Ref. 3. See original work.
[k]Reference 8.
[l]The A_0, B_0, and C_0 values were evaluated using the r_0 geometrical parameters derived in Ref. 8.
[m]Reference 9.

electrons being included in the correlation treatment, agree reasonably well with the best estimated and available experimentally derived values discussed above.

V. OPTIMIZED GEOMETRICAL PARAMETERS OF THE $\tilde{A}\ ^2A_1$ STATE OF AsH_2

Similar to the $\tilde{X}\ ^2B_1$ state discussed above, basis set size effects on both computed RCCSD(T) r_e and θ_e values of the $\tilde{A}\ ^2A_1$ state of AsH_2 (employing the AVQZ and AV5Z basis sets) are small (see Table IV). Core correlation effects from the As $3d^{10}$ electrons {RCCSD(T)/ACV5Z values compared with RCCSD(T)/AV5Z values} change computed r_e and θ_e values by −0.0134 Å and +0.24°, respectively. The best estimated r_e geometrical parameters for the $\tilde{A}\ ^2A_1$ state are 1.4787 ± 0.0001 Å and $122.01° \pm 0.01°$ (see footnote c of Table IV), which can be compared with the available experimental r_e values of 1.498 ± 0.003 Å and $121.66 \pm 0.02°$ derived from the CRD study of Ref. 9. Similarly, the best estimated computed r_0 geometrical parameters of 1.4825 Å and 122.16°, and rotational constants of A_0=16.710 cm^{-1}, B_0 =4.967 cm^{-1}, and C_0=3.829 cm^{-1} can be compared with available, corresponding experimental values of approximately 1.483 Å, 123.0°–123.1°, 17.207–17.191 cm^{-1},

Downloaded 10 Jan 2012 to 158.132.161.9. Redistribution subject to AIP license or copyright; see http://jcp.aip.org/about/rights_and_permissions

TABLE IV. Computed minimum-energy geometrical parameters (r_e and θ_e in angstrom and degrees, respectively; r_0 values are specified under method) and the corresponding rotational constants (A, B, and C in cm^{-1}) of the $\tilde{A}\ ^2A_1$ state of AsH_2.

Method	r_e	θ_e	A	B	C
RCCSD(T)/AVQZ	1.4921	121.74			
RCCSD(T)/AV5Z	1.4921	121.76			
RCCSD(T)/ACV5Z	1.4787	121.99			
CBS[a]	1.4921	121.77			
Core[b]	−0.0134	+0.237			
Best estimate[c]	1.4787(1)	122.01(1)	16.716	5.000	3.849
RCCSD(T)/AV5Z PEF	1.4920	121.95	16.388	4.914	3.780
RCCSD(T)/AV5Z PEF r_0	1.5000	122.09	16.284	4.855	3.740
RCCSD(T)/ACV5Z PEF	1.4787	122.18	16.804	4.991	3.848
RCCSD(T)/ACV5Z PEF r_0	1.4825	122.33	16.706	4.931	3.807
Best r_0 [d]	1.4825	122.16	16.710	4.967	3.829
RHF/UCCSD(T)-F12b/$AVTZ_{ae}$	1.4962	121.77	16.201	4.894	3.759
RHF/UCCSD(T_{sc})-F12b/$AVQZ_{ae}$	1.4960	121.78	16.211	4.895	3.760
RHF/UCCSD(T_{sc})-F12a/AVTZ	1.4934	121.74	16.250	4.914	3.773
RHF/UCCSD(T)-F12a/AVTZ	1.4931	121.73			
RHF/UCCSD(T_{sc})-F12b/AVTZ	1.4930	121.73			
RHF/UCCSD(T)-F12b/AVTZ	1.4929	121.73			
RHF/UCCSD(T)-F12b/ACVTZ	1.4823	121.94			
RHF/UCCSD(T_{sc})-F12a/ACVTZ	1.4818	121.99	16.635	4.980	3.833
RHF/UCCSD(T_{sc})-F12a/ACVTZ PEF	1.4815	122.13			
(as above) r_0	1.4897	122.27	16.604	4.914	3.792
UCCSD(T)/aug-cc-pVQZ[e]	1.474	122.2			
Absorption r_0 [f]	1.48	123.0			
LIF r_0 [g]	1.4830(1)	123.10(2)	17.2065(1)	4.919 567(7)	3.740 424(7)
CRD absorption r_0 [h]	1.4834(1)	123.084(7)	17.1908(4)	4.9178(3)	3.7407(3)
CRD absorption[h]	1.498(3)	121.66(2)			

[a]Extrapolation to the CBS limit using the $1/X^3$ formula and the RCCSD(T)/AVQZ and RCCSD(T)/AV5Z values.
[b]Contributions from As $3d^{10}$ outer core correlation take the difference between the computed RCCSD(T)/ACV5Z values, which include the As $3d^{10}$ electrons in the correlation calculations, and the RCCSD(T)/AV5Z values, with the default frozen core.
[c]The best estimated values take the sums of the CBS values and core contribution (i.e., CBS+core). The uncertainties are estimated by the difference between the best estimates and the RCCSD(T)/ACV5Z values.
[d]The best r_0 values are estimated by the sums of the best estimated r_e values and the differences between the r_0 and r_e values obtained from the RCCSD(T)/ACV5Z PEF.
[e]From Ref. 8 using G03.
[f]Reference 4.
[g]Reference 8.
[h]Reference 9.

4.918–4.920 cm^{-1}, and 3.740–3.741 cm^{-1}. The agreement between theory and experiment can still be considered as reasonably good, though not as good as for the $\tilde{X}\ ^2B_1$ state. Nevertheless, the most important conclusion on the geometrical structure of the $\tilde{A}\ ^2A_1$ state of AsH_2 in relation to its $\tilde{A}$-$\tilde{X}$ emission spectrum is that, the major geometry change upon deexcitation between the $\tilde{X}\ ^2B_1$ and $\tilde{A}\ ^2A_1$ states is a large decrease in the equilibrium bond angle. Specifically, the best theoretical estimates from the present study give $\Delta\theta_e$ and $\Delta\theta_0$ values upon deexcitation of approximately 31.2°, while the CRD study[9] recommends a $\Delta\theta_e$ value of approximately 30.9°, and both the LIF/DF (Ref. 8) and absorption[4] studies yield a $\Delta\theta_0$ value of approximately 32.3°. In this connection, it is concluded that theory, based on high-level *ab initio* calculations of the present work, and experiment, based on rotational analyses of high-resolution electronic spectra of Refs. 4, 8, and 9, agree in an increase of bond angle of approximately 31.5° ± 0.8° (the average of 31.2°, 30.9°, and 32.3°) upon excitation from the $\tilde{X}\ ^2B_1$ state to the $\tilde{A}\ ^2A_1$ state. In Ref. 8, this large increase in the bond angle upon excitation has been attributed to the different bonding character of the different singly occupied molecular orbitals of, and the different electron density distributions in, the two electronic states of AsH_2.

Considering computed UCCSD(T)-F12x results for the $\tilde{A}\ ^2A_1$ state of AsH_2 (see Table IV), the observed trends are very similar to those observed for the $\tilde{X}\ ^2B_1$ state discussed above, and hence will not be repeated here. Summarizing, the computed UCCSD(T)-F12x/ACVTZ geometrical parameters agree very well with the best estimates based on RCCSD(T) results discussed above. It should be noted that a single energy calculation at the RCCSD(T)/ACV5Z level takes approximately 17 times more CPU time than a calculation at the UCCSD(T)-F12x/ACVTZ level. It is therefore concluded that the simplified explicitly correlated UCCSD(T)-F12x methods are very attractive alternatives to conventional correlation methods, because they are computationally, considerably less expensive (by employing a smaller AO basis set), but appear to be as reliable (see also later text).

Downloaded 10 Jan 2012 to 158.132.161.9. Redistribution subject to AIP license or copyright; see http://jcp.aip.org/about/rights_and_permissions

TABLE V. Computed and experimental vibrational frequencies {harmonic $\omega_1(a_1)$, $\omega_2(a1)$, and $\omega_3(b_2)$; [fundamental ν_1, ν_2, and ν_3] in cm^{-1}} of the $\tilde{X}\ ^2B_1$ and $\tilde{A}\ ^2A_1$ states of AsH_2.

$\tilde{X}\ ^2B_1$	$\omega_1(a_1)$	$\omega_2(a1)$	$\omega_3(b_2)$
RCCSD(T)/AVQZ	2175.8	1003.6	2185.6
RCCSD(T)/AV5Z PEF	2177.9 [2131.5]	1001.1 [996.6]	
RCCSD(T)/ACV5Z PEF	2200.6 [2151.7]	1015.3 [1006.7]	
RHF/UCCSD(T)-F12b/$AVTZ_{ae}$	2185.8	1000.8	2194.0
RHF/UCCSD(T_{sc})-F12a/AVTZ	2172.3	1001.6	2182.6
RHF/UCCSD(T_{sc})-F12a/ACVTZ	2187.2	1008.4	2200.1
RHF/UCCSD(T_{sc})-F12a/ACVTZ PEF	2186.8 [2139.9]	1005.3 [1000.6]	
UCCSD(T)/aug-cc-pVQZ[a]	2186	1027	2198
Emission[b]		987 [985]	
SVL[c] ω^0s[ν's]	2096.5(9) [2095.1]	984.5(6) [981.4]	
SVL[c,d]		987.39	
CRD absorption[e]		981.37 [981.368(3)]	
$\tilde{A}\ ^2A_1$			
RCCSD(T)/AVQZ	2229.4	865.3	2334.8
RCCSD(T)/AV5Z PEF	2231.2 [2170.2]	871.0 [864.0]	
RCCSD(T)/ACV5Z PEF	2255.5 [2193.9]	864.5 [867.4]	
RHF/UCCSD(T)-F12b/$AVTZ_{ae}$	2249.5	858.6	2345.3
RHF/UCCSD(T_{sc})-F12a/AVTZ	2220.8	864.1	2327.2
RHF/UCCSD(T_{sc})-F12a/ACVTZ	2238.0	867.7	2349.2
RHF/UCCSD(T_{sc})-F12a/ACVTZ PEF	2240.5 [2177.3]	867.5 [865.2]	
UCCSD(T)/aug-cc-pVQZ[a]	2265	881	2361
Absorption[b]		855.0 [851.4]	
Emission[f]		[867]	
LIF[c] ω^0s[ν's]	2112.7(1) [2112.71]	852.4(2) [850.43]	
LIF[b,c]		854.00	
CRD absorption[e]		854.28 [850.345(3)]	

[a]From Ref. 8.
[b]Reference 4.
[c]Reference 8.
[d]The ω_2 values of the two states were obtained by refitting results of Ref. 8 by a different expansion; see Ref. 9.
[e]Reference 9.
[f]Reference 5.

VI. COMPUTED VIBRATIONAL FREQUENCIES OF THE $\tilde{X}\ ^2B_1$ AND $\tilde{A}\ ^2A_1$ STATES OF AsH_2

Computed harmonic and fundamental vibrational frequencies of the $\tilde{X}\ ^2B_1$ and $\tilde{A}\ ^2A_1$ states of AsH_2 obtained at different levels are summarized in Table V. At the RCCSD(T)/AV5Z, RCCSD(T)/ACV5Z and UCCSD(T_{sc})-F12a/ACVTZ levels, anharmonic vibrational wave functions have been computed (see Table II), and some of the calculated fundamental and higher excited vibrational energies are presented, and compared with available experimental values, in Table VI. From Table V, the largest difference in the computed vibrational frequencies (among all the ω and ν values shown) obtained at different levels of calculation in the present study is approximately 35 cm^{-1} {i.e., the difference between the UCCSD(T_{sc})-F12a/ACVTZ ω_1 and RCCSD(T)/ACV5Z PEF ω_1 values of the $\tilde{A}\ ^2A_1$ state in Table V; the UCCSD(T_{sc})-F12a/AVTZ values are generally in between the RCCSD(T)/AV5Z and RCCSD(T)/ACV5Z values}. This may be considered as a reasonable estimate of the uncertainties associated with the computed vibrational frequencies obtained in this work. Comparing computed and experimental fundamental vibrational frequencies of the two states of AsH_2 shown in Table V, the relatively smaller computed RCCSD(T)/AV5Z values seem to agree better with available experimental values than the corresponding RHF/UCCSD(T_{sc})-F12a/ACVTZ and RCCSD(T)/ACV5Z values. However, from Table VI, and as will be discussed later concerning the comparison between simulated and experimental $\tilde{A}(0,0,0)$-$\tilde{X}$ SVL emission spectra of AsH_2, the RCCSD(T)/ACV5Z results seem to agree with experiment better than the RCCSD(T)/AV5Z results for higher excited vibrational levels, particularly for the $\tilde{X}\ ^2B_1$ state. The differences between the computed RCCSD(T)/ACV5Z and experimental ν_1 and ν_2 fundamental vibrational frequencies are approximately 56 and 34 cm^{-1} for the $\tilde{X}\ ^2B_1$ state and 81 and 17 cm^{-1} for the $\tilde{A}\ ^2A_1$ state, respectively. The overall agreement between theory and experiment in the vibrational frequencies of the two states of AsH_2 can only be considered as fair, particularly for the symmetric stretching ν_1 modes of both states (in the case of ν_1, the poorer agreement between theory and experiment, cf. ν_2, may be due to MR character in the large bond length region of the symmetric stretching potential energy surface). Nevertheless, as mentioned above and noted in Ref. 8, anharmonicity for the symmetric stretching ν_1 mode of AsH_2 is expected to be substantial, as As is considerably heavier than H. The computed fundamental fre-

Downloaded 10 Jan 2012 to 158.132.161.9. Redistribution subject to AIP license or copyright; see http://jcp.aip.org/about/rights_and_permissions

TABLE VI. Comparison between available experimental {Em, absor, and CRD refer to emission (Ref. 4), absorption (Ref. 5), and CRD absorption (Ref. 9) studies; ΔG is the separation between adjacent (i.e., v_2 and v_2-1) vibrational levels} and computed vibrational energies (in cm^{-1}) of the $\tilde{X}\ ^2B_1$ and $\tilde{A}\ ^2A_1$ states of AsH_2 obtained using the RCCSD(T)/AV5Z and RCCSD(T)/ACV5Z PEFs.

$\tilde{X}$	SVL	ΔG	AV5Z	ΔG	ACV5Z	ΔG	Em				CRD	
2_1	981.4		996.5		1006.7		985				981.4	
2_2	1953.0	971.6	1986.5	990.0	2004.8	990.5	1962	977				
2_3	2918.7	965.0	2966.9	980.4	2995.3	990.5						
2_4	3875.7	957.0	3934.0	967.1	3977.8	982.5						
2_5	4824.8	949.1	4883.0	949.0	4951.1	973.3						
2_6	5763.9	939.1	5805.8	922.8	5913.2	962.1						
2_7	6693.1	929.2	6685.0	879.2	6861.8	948.6						
2_8	7609.5	916.4	7448.0	763.0[a]	7793.4	931.6						
2_9	8516.8	907.3	8262.8	814.8[a]	8703.0	909.6						
1_1	2095.1		2131.5		2151.7							
1_12_1	3060.4	965.3	3112.4	980.9	3143.1	991.4						
1_12_2	4020.4	960.0	4087.1	974.7	4125.7	982.6						
1_12_3	4969.4	949.0	5052.5	965.4	5100.7	975.0						
1_12_4	5910.9	941.5	6004.1	951.6	6067.7	967.0						
1_12_5	6840.9	930.0	6936.3	932.2	7025.2	957.5						
1_12_6	7763.4	922.5	7834.5	898.2	7971.3	946.1						
1_12_7	8975.1	1211.7[a]	8721.9	887.4	9059.3	1088[a]						
$\tilde{A}$	LIF	ΔG	AV5Z	ΔG	ACV5Z	ΔG	Em	ΔG	Absor	ΔG	CRD	ΔG
2^1	850.43		864.0		867.4		866		851.4		850.345	
2^2	1695.86	845.43	1719.7	855.7	1730.2	862.8	1736	870	1696.8	845.4	1695.856	845.51
2^3	2535.41	839.55	2567.6	847.9	2583.2	853.0	2579	843	2536.4	839.6	2535.597	839.74
2^4	3368.33	832.92	3406.8	839.2	3422.8	839.6	3426	847	3195.4	832.5		
2^5	4192.80	824.47	4234.5	827.7	4245.6	822.8			4195.4	826.5		
2^6			5045.3	810.8	5045.0	799.4			5015.9	820.5		
1^1	2112.71		2170.2		2193.9							
1^12^1	2948.67	835.96	3022.0	851.8	3048.9	855.0						

[a]These separations do not fit with the trend, and hence the assignments are doubtful.

quencies are slightly larger than the experimental ones in all cases, suggesting slight underestimations of anharmonicities in the variational calculations of anharmonic vibrational wave functions of both states of AsH_2, when anharmonic vibrational wave functions are expressed in terms of linear combinations of harmonic basis functions. Nevertheless, the largest discrepancy between computed and experimental fundamental frequencies (ν_1') is less than 4% of the experimental value, which may be considered as acceptable.

VII. COMPUTED RELATIVE ELECTRONIC ENERGIES

From Table VII, the best estimated T_e value of the $\tilde{A}\ ^2A_1$ state of AsH_2 (with respect to the $\tilde{X}\ ^2B_1$ state) obtained from the present study based on a series of RCCSD(T) calculations is $19\,922.15 \pm 29.2$ cm^{-1} (2.4700 ± 0.0037 eV; see footnote c of Table VII). Including corrections for zero-point energies of the two states involved (ΔZPE; see footnote d of Table VII), the best estimated T_0 value is $19\,954.4$ cm^{-1} (2.4740 eV). Comparing this value with available experimental T_0 values of $19\,909.4531(18)$ and $19\,909.4910(17)$ cm^{-1} (both equivalent to 2.4685 eV) from the LIF (Ref. 8) and CRD (Ref. 9) studies, it is pleasing that the agreement between theory and experiment is better than 45 cm^{-1} (0.006 eV). This is a considerable improvement from the previously highest level, UCCSD(T)/aug-cc-pVQZ T_e value of $19\,168$ cm^{-1} (2.3765 eV) of Ref. 8, which is smaller than the experimental T_0 values by 741 cm^{-1} (0.092eV).

Considering the computed UCCSD(T)-F12x relative electronic energies shown in Table VII, it is clear that relativistic contributions, as accounted for by employing the fully relativistic ECP, are important in the evaluation of the $\tilde{A}$-$\tilde{X}$ relative electronic energy of AsH_2. This is shown in the differences between computed UCCSD(T)-F12x T_e values obtained employing the all electron basis sets ($AVTZ_{ae}$ and $AVQZ_{ae}$) and the ECP basis sets (AVTZ and ACVTZ). Specifically, with the all electron basis sets, the computed UCCSD(T)-F12x T_e values are of similar magnitudes (approximately $19\,100$ cm^{-1}) to the UCCSD(T)/aug-cc-pVQZ T_e value of Ref. 8 ($19\,168$ cm^{-1}), and are approximately 800 cm^{-1} smaller than the experimental T_0 values[8,9] of approximately $19\,909$ cm^{-1}. With the AVTZ ECP basis set, the various computed UCCSD(T)-F12x T_e values increase to between $19\,796$ and $19\,831$ cm^{-1}. With the ACVTZ ECP basis set, and the As $3d^{10}$ core electrons being correlated, the various computed UCCSD(T)-F12x T_e values increase further to between $19\,909$ and $19\,935$ cm^{-1}, which agree very well with the best estimated theoretical T_e value of $19\,922$ cm^{-1} and experimental T_0 value of $19\,909$ cm^{-1}. In addition, it can be seen from Table VII that the differences between the two F12x (x=a or b) approximations are small at least as far as computed relative electronic energies are concerned.

Downloaded 10 Jan 2012 to 158.132.161.9. Redistribution subject to AIP license or copyright; see http://jcp.aip.org/about/rights_and_permissions

TABLE VII. Computed electronic energies (T_e; otherwise specified under Method) of the $\tilde{A}\ ^2A_1$ state of AsH_2 relative to the $\tilde{X}\ ^2B_1$ state obtained at different levels of calculation.

Method	T_e (cm^{-1})	T_e (eV)
RCCSD(T)/AVQZ	19 832.5	2.4589
RCCSD(T)/AV5Z	19 804.7	2.4555
RCCSD(T)/ACV5Z	19 951.3	2.4737
CBS[a]	19 775.5 ± 29.2	2.4519 ± 0.0036
Core[b]	+146.6	+0.0182
Best estimate[c]	19 922.15 ± 29.2	2.4700 ± 0.0037
Δ(ZPE) [d]	+32.2	+0.0040
Best T_0=best T_e+Δ(ZPE) [d]	19 954.4 ± 32.4	2.4740 ± 0.0040
RHF/UCCSD(T)-F12b/$AVTZ_{ae}$	19 155.4	2.3749
RHF/UCCSD(T_{sc})-F12b/$AVQZ_{ae}$	19 086.0	2.3664
RHF/UCCSD(T_{sc})-F12a/AVTZ	19 795.6	2.4543
RHF/UCCSD(T)-F12a/AVTZ	19 814.6	2.4567
RHF/UCCSD(T_{sc})-F12b/AVTZ	19 813.0	2.4565
RHF/UCCSD(T)-F12b/AVTZ	19 831.9	2.4589
DF-RMP2-F12//RHF/UCCSD(T)-F12b/ACVTZ	19 904.7	2.4679
RHF/UCCSD-F12a//RHF/UCCSD(T)-F12b/ACVTZ	20 070.9	2.4885
RHF/UCCSD(T)-F12a//RHF/UCCSD(T)-F12b/ACVTZ	19 917.8	2.4694
RHF/UCCSD-F12b//RHF/UCCSD(T)-F12b/ACVTZ	20 071.7	2.4886
RHF/UCCSD(T)-F12b/ACVTZ	19 935.2	2.4717
DF-RMP2-F12//RHF/UCCSD(T_{sc})-F12a/ACVTZ	19 905.6	2.4680
RHF/UCCSD-F12a//RHF/UCCSD(T_{sc})-F12a/ACVTZ	20 070.9	2.4885
RHF/UCCSD(T_{sc})-F12a/ACVTZ	19 908.5	2.4683
RHF/UCCSD-F12b//RHF/UCCSD(T_{sc})-F12a/ACVTZ	20 071.7	2.4886
RHF/UCCSD(T_{sc})-F12b//RHF/UCCSD(T_{sc})-F12a/ACVTZ	19 909.4	2.4684
UCCSD(T)/aug-cc-pVQZ[e]	19 168	2.3765
Absorption T_0 [f]	19 905.5	2.4680
Emission T_0 [g]	19 928	2.4708
LIF T_0 [h]	19 909.4531(18)	2.4685
CRD absorption T_0 [i]	19 909.4910(17)	2.4685

[a]Extrapolation to the CBS limit using the $1/X^3$ formula and the RCCSD(T)/AVQZ and RCCSD(T)/AV5Z values. The estimated uncertainties take the difference between the CBS and RCCSD(T)/AV5Z values.
[b]Contributions from As $3d^{10}$ outer core correlation take the difference between the computed RCCSD(T)/ACV5Z values, which include As $3d^{10}$ electrons in the correlation calculations, and the RCCSD(T)/AV5Z values, with the default frozen core.
[c]The best estimated values take the sums of the CBS values and Core contribution (i.e., CBS+Core). The uncertainties are estimated by the difference between the best estimates and the RCCSD(T)/ACV5Z values.
[d]Zero-point energy corrections employing the computed harmonic vibrational frequencies of the two states obtained at the RCCSD(T)/AVQZ level of calculation (Table IV). A 10% uncertainty is assumed in Δ(ZPE) to give the overall uncertainties as shown for the best estimated T_0 values.
[e]From Ref. 8.
[f]Reference 4.
[g]Reference 5.
[h]Reference 8.
[i]Reference 9.

However, if the triple excitations are not included, whether scaled or unscaled, the computed T_e values are larger, in the approximately 20 070 cm^{-1} region. Summarizing, it is concluded that contributions from relativistic effects, core correlation and triple excitations are important in the evaluation of relative electronic energies of AsH_2. Nevertheless, the differences between the two F12x (x=a or b) approximations, and between scaled and unscaled triples, are small. Lastly, it should be mentioned that the computed DF-RMP2-F12//RHF/UCCSD(T)-F12b/ACVTZ and DF-RMP2-F12//RHF/UCCSD(T_{sc})-F12a/ACVTZ T_e values of 19 904.7 and 19 905.6 cm^{-1}, respectively, agree very well with the experimental T_0 values of approximately 19 909 cm^{-1}, suggesting that the density-fitted explicitly correlated MP2 method (DF-RMP2-F12) may be an even more cost-effective method than the more elaborate UCCSD(T)-F12x method.

VIII. SIMULATED $\tilde{A}(0,0,0)$-$\tilde{X}$ SVL EMISSION SPECTRA OF AsH_2

Before simulated spectra are discussed, it should be noted that the best estimated geometrical parameters of the two states involved, obtained in the present study, have been employed in FC factor calculations, thus giving the best theoretical simulated spectra, unless otherwise stated. In any case, the best estimated geometry changes (Δr_e and/or Δr_0 geometrical parameters) of the two states of AsH_2 upon de-excitation obtained in the present study are very similar to those derived experimentally from Refs. 4, 8, and 9 (for instance, the best estimated Δr_e and $\Delta\theta_e$ values differ only by approximately 0.006 Å and 0.3° from the corresponding, experimental values derived in the CRD study[9]), as mentioned above. Nevertheless, the geometry, particularly the bond

Downloaded 10 Jan 2012 to 158.132.161.9. Redistribution subject to AIP license or copyright; see http://jcp.aip.org/about/rights_and_permissions

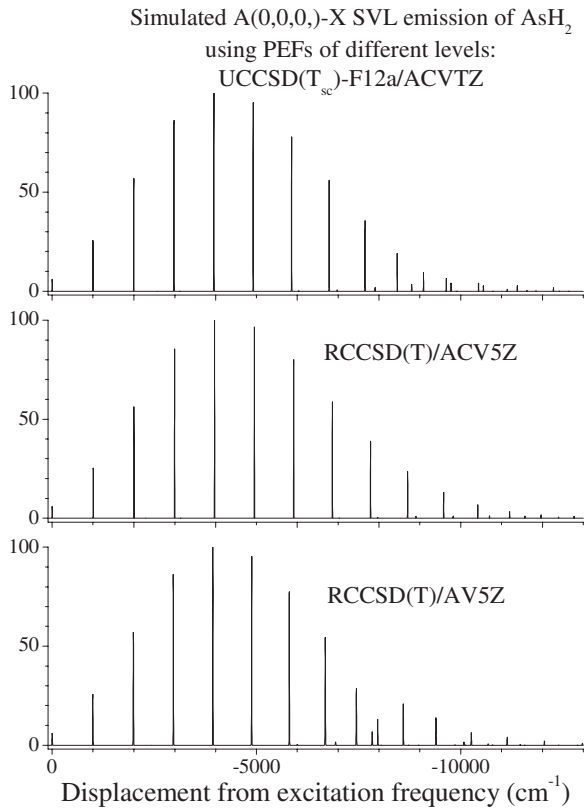

FIG. 1. Simulated $\tilde{A}\ ^2A_1(0,0,0) \rightarrow \tilde{X}\ ^2B_1$ SVL emission spectra of AsH_2 obtained employing three different sets of PEFs (the best estimated geometrical parameters of the two states were used in the FCF calculations and a FWHM of 5 cm^{-1} was used in the spectral simulation; see text).

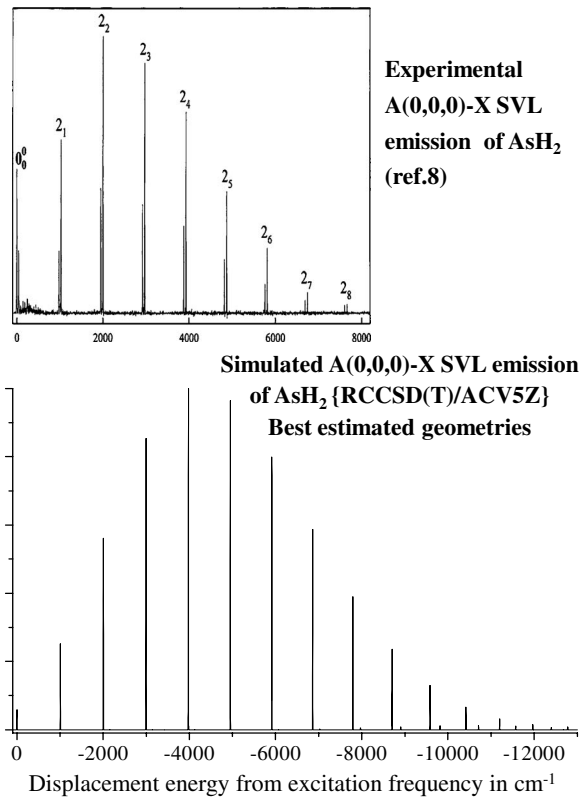

FIG. 2. Comparison between the experimental (top; note that the splitting in each vibrational component is due to partially resolved rotational structure; see Ref. 8) and simulated (bottom) $\tilde{A}\ ^2A_1(0,0,0) \rightarrow \tilde{X}\ ^2B_1$ SVL emission spectra of AsH_2 employing the best theoretical geometrical parameters of the two states (see text).

angle of the $\tilde{A}\ ^2A_1$ state of AsH_2 will be further discussed, when simulated and experimental $\tilde{A}(0,0,0)$-$\tilde{X}$ SVL emission spectra are compared below.

First, simulated spectra obtained employing three different sets of PEFs are compared in Fig. 1. It can be seen that the three simulated spectra are very similar. Only slight differences are found in the low emission energy region (large displacement energy from the excitation frequency; less than -7000 cm^{-1} in Fig. 1) of the simulated spectrum obtained employing the RCCSD(T)/AV5Z PEFs for the two states (bottom trace in Fig. 1), when compared with the other two simulated spectra. Specifically, with the set of RCCSD(T)/AV5Z PEFs, vibrational components to $(0,v_2'',0)$ and $(1,v_2''\text{-}2,0)$ levels, with $v_2'' \geq 8$, appear to have stronger mixings than those with the other two sets of PEFs. Theoretically, the RCCSD(T)/ACV5Z and UCCSD(T_{sc})-F12a/ACVTZ PEFs should be superior to the RCCSD(T)/AV5Z PEFs, as the former PEFs have included As $3d^{10}$ core correlation, but the latter PEF has not. Also, comparisons between simulated and experimental $\tilde{A}(0,0,0)$-$\tilde{X}$ SVL emission spectra suggest that the agreement with the experimental spectrum (Fig. 2 top trace) is slightly poorer for the RCCSD(T)/AV5Z simulated spectrum in the low emission energy region than for the other two simulated spectra (middle and top traces in Fig. 1). As for the simulated $\tilde{A}(0,0,0)$-$\tilde{X}$ SVL emission spectra obtained employing the RCCSD(T)/ACV5Z and UCCSD(T_{sc})-F12a/ACVTZ PEFs, they are essentially identical up to approximately -9000 cm^{-1} displacement energy (Fig. 1, middle and top traces). For the sake of simplicity, we focus mainly on simulated spectra obtained with the RCCSD(T)/ACV5Z PEFs from here onwards.

The experimental $\tilde{A}(0,0,0)$-$\tilde{X}$ SVL emission spectrum of Ref. 8 is compared with the simulated spectrum obtained using the set of RCCSD(T)/ACV5Z PEFs for the two states in Fig. 2. Theory and experiment agree that there is only one main $(0,0,0)$-$(0,n_2'',0)$ vibrational series (the doublet structure for each vibrational component observed in the experimental spectrum is due to partially resolved rotational structure; see original work). However, a more detailed comparison reveals some discrepancies between the simulated and experimental spectra. Specifically, the 2_2 vibrational component has the maximum relative intensity in the experimental spectrum (top trace of Fig. 2), while the 2_4 vibrational component is the strongest in the simulated spectrum (bottom trace of Fig. 2). In addition, the changes in relative intensities of the vibrational components near the band maximum at the 2_2 vibrational component in the experimental spectrum seem to be rather large for 2_n components with $n \geq 3$, unlike the more smooth and gradual changes in the 2_n progression of the simulated spectrum. As discussed above, the computed and experimentally derived bond angle changes upon deexcitation agree with each other and are nearly 32°. In this connection, it seems more reasonable that the maximum relative intensity in the 2_n bending series occurs for the 2_4 component as in the simulated spec-

Downloaded 10 Jan 2012 to 158.132.161.9. Redistribution subject to AIP license or copyright; see http://jcp.aip.org/about/rights_and_permissions

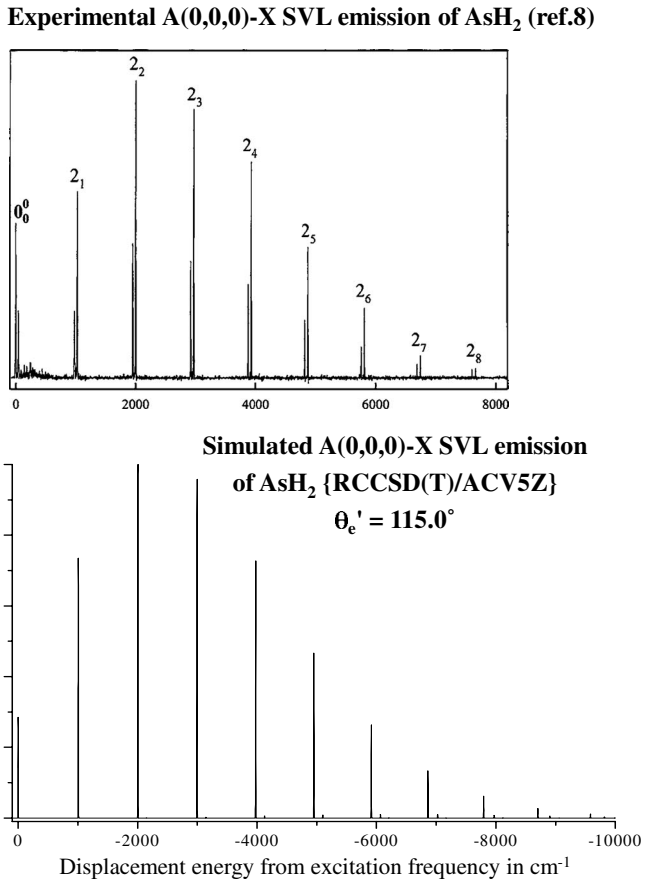

FIG. 3. Comparison between the experimental (top; note that the splitting in each vibrational component is due to partially resolved rotational structure; see Ref. 8) and simulated (bottom) $\tilde{A}\ ^2A_1(0,0,0) \rightarrow \tilde{X}\ ^2B_1$ SVL emission spectra of AsH_2 employing the best theoretical geometrical parameters of the two states, except for the θ_e' equilibrium bond angle of the $\tilde{A}\ ^2A_1$ state, which was set to 115.0°. (see text).

trum than for the 2_2 component as in the experimental spectrum. In order to obtain a simulated vibrational envelope, which has the 2_2 component as the strongest in the $\tilde{A}(0,0,0)$-$\tilde{X}$ SVL emission band, further FC factor calculations were carried out using smaller bond angles for the $\tilde{A}\ ^2A_1$ state. Simulated spectra thus obtained suggest that the bond angle change upon deexcitation has to be reduced to approximately 24°, i.e., the θ_e' value for the $\tilde{A}\ ^2A_1$ state would be approximately 115°, which is smaller than the best theoretical estimate and experimentally derived values by approximately 7°. A simulated spectrum obtained with $\theta_e' = 115.0°$ (the rest of the geometrical parameters used are the best estimates) is compared with the experimental spectrum in Fig. 3. Although the match between the simulated and experimental spectra in Fig. 3 may appear to be better than that in Fig. 2, the difference between a smooth and gradual change of relative intensities of successive vibrational components in the simulated spectrum and a larger intensity change in the experimental spectrum, as mentioned above, can still be seen in Fig. 3. Also, with the equilibrium geometry of the $\tilde{A}\ ^2A_1$ state of AsH_2 used to simulate the spectrum shown in Fig. 3 (bottom trace), the corresponding rotational constants have the following values: $A_e = 13.606$, $B_e = 5.377$, and $C_e = 3.854$ cm^{-1}, which are very different from corresponding, available experimental values derived from rotational analyses of some high-resolution electronic spectra (Refs. 4, 8, and 9; see Table IV). Summing up, state-of-the-art *ab initio* calculations and rotational analysis of high-resolution electronic spectra[4,8,9] agree that the θ_e' value should be approximately 122° and cannot be as small as 115°. In addition, it has been recently documented that dispersed fluorescence spectra recorded using a photomultiplier tube (PMT) as the detector (as in Ref. 8) could have reduced signals at low emission energies {cf. when a high sensitivity intensified charge-coupled device (ICCD) is used as the detector; see, for example, Ref. 30, where the SVL emissions of CCl_2 fluorescing from approximately 19 700 cm^{-1} to lower emission energies, in an energy region similar to the $\tilde{A}(0,0,0)$-$\tilde{X}$ SVL emission of AsH_2, were recorded using both a PMT and a ICCD}. It is therefore concluded that the discrepancies between the experimental $\tilde{A}(0,0,0)$-$\tilde{X}$ SVL emission spectrum and the best theoretical simulated spectrum is probably due to a loss of detector sensitivity toward low emission energies in the experimental spectrum (see also Ref. 31).

IX. CONCLUDING REMARKS

State-of-the-art *ab initio* calculations have been carried out on the $\tilde{X}\ ^2B_1$ and $\tilde{A}\ ^2A_1$ states of AsH_2, employing the established correlation method, RCCSD(T), and two simplified versions of the explicitly correlation method, UCCSD(T)-F12x, where x=a or b. With the conventional RCCSD(T) method, basis sets of up to quintuple-zeta quality were used and extrapolation to the CBS limit was carried out. In addition, relativistic effects were accounted for by employing a fully relativistic ECP for As, and core correlation of the As $3d^{10}$ electrons was included explicitly with a tight set of 4d3f2g2h functions added to the ECP10MDF_AV5Z basis set. It is pleasing that with this conventional approach, the best estimated relative electronic energy between the $\tilde{A}\ ^2A_1$ and $\tilde{X}\ ^2B_1$ states of AsH_2 obtained, which is supposed to be one of the most demanding quantities (cf. geometry and vibrational frequencies as considered in a composite method) to be computed in an *ab initio* manner, agrees with highly reliable experimental values to within 45 cm^{-1} (0.0056 eV). With the simplified explicitly correlated methods, UCCSD(T)-F12x, it has been found that the differences between the two versions, F12a and F12b, and also between including scaled and unscaled triples, are small. In addition, we have employed ECP basis sets for As and also correlated As $3d^{10}$ electrons explicitly in UCCSD(T)-F12x calculations for the first time. It was found that with a core-valence triple-zeta quality ECP basis set and As $3d^{10}$ electrons being correlated, UCCSD(T)-F12x results are comparable with the best estimated results obtained based on RCCSD(T) calculations employing quadruple- and quintuple-zeta basis sets and extrapolation to the CBS limit. Since these UCCSD(T)-F12x calculations have employed a smaller basis set than the RCCSD(T) calculations, they require only a fraction of the computational cost when compared with the RCCSD(T) calculations. As a bonus, it was found that the DF-RMP2-F12 method also performs very

Downloaded 10 Jan 2012 to 158.132.161.9. Redistribution subject to AIP license or copyright; see http://jcp.aip.org/about/rights_and_permissions

well regarding computed relative electronic energies. In this connection, explicitly correlated methods, such as DF-RMP2-F12 and UCCSD(T)-F12x, are clearly very attractive alternatives to conventional correlation methods, particularly for larger molecular systems. It is anticipated that these explicitly correlated methods will replace conventional correlated methods in the near future, as a matter of choice.

We have also computed PEFs for the two states of AsH_2 at different *ab initio* levels, which were used in variational calculations of anharmonic vibrational wave functions, which were in turn used in FC factor calculations between the two states of AsH_2. It is pleasing that simulated emission spectra obtained with the computed UCCSD(T_{sc})-F12a/ACVTZ PEFs are almost identical to corresponding simulated spectra obtained with the computationally much more demanding RCCSD(T)/ACV5Z PEFs. Again, this suggests that explicitly correlated methods can be used to generate reliable PEFs *in lieu* of conventional correlated methods at a considerably reduced cost.

Regarding the geometrical parameters of the $\tilde{X}\ ^2B_1$ and $\tilde{A}\ ^2A_1$ states of AsH_2, and the geometry changes upon excitation/deexcitation between the two states, it is concluded that theory and experiment agree very well, and these values are now firmly established as a result of the present study. In this connection, comparison between simulated and experimental $\tilde{A}(0,0,0)$-$\tilde{X}$ SVL emission spectra suggests that there is a significant loss in intensity in the low emission energy region of the experimental spectrum. Further investigations are required to clarify the discrepancies between the simulated and experimental spectra reported in the present study. Experimentally, employing a high sensitivity ICCD as the detector to record the dispersed fluorescence spectrum of AsH_2 (see Ref. 30) would ascertain the reliability of the experimental SVL emission spectrum reported in Ref. 8. Computationally, including dipole moment variation over the simulated spectral band, which has been ignored in the present study, may improve the agreement between the simulated and observed spectra.

ACKNOWLEDGMENTS

Financial support from the Research Grant Council (RGC) of the Hong Kong Special Administrative Region (HKSAR, Grant No. PolyU 5003/09P) is acknowledged. The authors are also grateful to the provision of computational resources from the EPSRC (U.K.) National Service for Computational Chemistry Software.

[1] M. Povey, D. Whitehead, K. Thomas, M. E. Pemble, M. Bardosova, and J. Renard, Appl. Phys. Lett. **89**, 104103 (2006).
[2] L. Dong, Q.-Q. Sun, Y. Shi, H. Liu, C. Wang, S.-J. Ding, and D. W. Zhang, Appl. Phys. Lett. **92**, 111105 (2008).
[3] R. Hughes, J. M. Brown, and K. M. Evenson, J. Mol. Spectrosc. **200**, 210 (2000).
[4] R. N. Dixon, G. Duxbury, and H. M. Lamberton, Proc. R. Soc. London, Ser. A **305**, 271 (1968).
[5] T. Ni, Q. Lu, X. Ma, S. Yu, and F. Kong, Chem. Phys. Lett. **126**, 417 (1986).
[6] H. Fujiwara, K. Kobayashi, H. Ozeki, and S. Saito, J. Phys. Chem. **109**, 5351 (1998).
[7] H. Fujiwara and S. Saito, J. Mol. Spectrosc. **192**, 399 (1998).
[8] S.-G. He and D. J. Clouthier, J. Chem. Phys. **126**, 154312 (2007).
[9] D. Zhao, C. Qin, M. Ji, Q. Zhang, and Y. Chen, J. Mol. Spectrosc. **256**, 192 (2009).
[10] L. Alberts and N. C. Handy, J. Chem. Phys. **89**, 2107 (1988).
[11] K. Balasubramanian, J. Chem. Phys. **91**, 2443 (1989).
[12] R. C. Binning and L. A. Curtiss, J. Chem. Phys. **92**, 1860 (1990).
[13] P. M. Mayer, J.-F. Gal and L. Radom, Int. J. Mass Spectrom. Ion Process. **167–168**, 689 (1997).
[14] C. W. Bock, K. D. Dobbs, G. J. Mains, and M. Trachtman, J. Phys. Chem. **95**, 7668 (1991).
[15] S. Hirata, T. Yanai, W. A. de Jong, T. Nakajima, and K. Hirao, J. Chem. Phys. **120**, 3297 (2004).
[16] P.-D. Fan and S. Hirata, J. Chem. Phys. **124**, 104108 (2006).
[17] P. J. Knowles, C. Hampel, and H.-J. Werner, J. Chem. Phys. **99**, 5219 (1993); **112**, 3106 (2000).
[18] MOLPRO2009, a package of *ab initio* programs written by H.-J. Werner and P. J. Knowles, version 2009.1, R. D. Amos, A. Bernhardsson, A. Berning *et al.*.
[19] B. Metz, H. Stoll, and M. Dolg, J. Chem. Phys. **113**, 2563 (2000).
[20] K. A. Peterson, J. Chem. Phys. **119**, 11099 (2003).
[21] T. H. Dunning, Jr., J. Chem. Phys. **90**, 1007 (1989).
[22] E. P. F. Lee, J. M. Dyke, F.-T. Chau, W. K. Chow, and D. K. W. Mok, J. Chem. Phys. **125**, 064307 (2006).
[23] A. Halkier, T. Helgaker, W. Klopper, P. Jorgensen, and A. G. Csaszar, Chem. Phys. Lett. **310**, 385 (1999).
[24] G. Knizia, T. B. Adler, and H.-J. Werner, J. Chem. Phys. **130**, 054104 (2009).
[25] T. Helgaker, W. Klopper, and D. P. Tew, Mol. Phys. **106**, 2107 (2008).
[26] See: http://www.molpro.net/info/users?portal=user for online MOLPRO User Manual.
[27] D. K. W. Mok, F.-T. Chau, E. P. F. Lee, and J. M. Dyke, ChemPhysChem **6**, 719 (2005).
[28] D. K. W. Mok, E. P. F. Lee, F.-T. Chau, D. C. Wang, and J. M. Dyke, J. Chem. Phys. **113**, 5791 (2000).
[29] J. Demaison, Mol. Phys. **105**, 3109 (2007).
[30] M.-L. Liu, C.-L. Lee, A. Bezant, G. Tarczay, R. J. Clark, T. A. Miller, and B.-C. Chang, Phys. Chem. Chem. Phys. **5**, 1352 (2003).
[31] J. M. Dyke, E. P. F. Lee, D. K. W. Mok, W.-K. Chow, and F.-T. Chau, ChemPhysChem **6**, 2046 (2005).

Downloaded 10 Jan 2012 to 158.132.161.9. Redistribution subject to AIP license or copyright; see http://jcp.aip.org/about/rights_and_permissions